2023 62nd IEEE Conference on Decision and Control (CDC)
December 13-15, 2023. Marina Bay Sands, Singapore

Exploiting resource constraints for controlling biomolecular circuits

Abhilash Patel, Guy-Bart Stan

***Abstract*— Advances in synthetic biology depend on our ability to predictably engineer robust biomolecular systems in living cells. The functioning of these synthetic biomolecular systems requires the consumption of shared cellular resources, which imposes a gene expression burden that may impact the performance of the cell and the synthetic system. In this paper, we show the effect of resource constraints on quantitative and qualitative aspects of gene expression in multiple circuits. We utilise a resource-aware modelling framework to show that stabilization can be achieved in a class of integral controllers. The results open possibilities for the design of lean biomolecular controllers.**

I. Introduction

Designing biomolecular systems in living cells for eventual applications in agriculture, healthcare, and industry is an important aspect of synthetic biology. These engineered biomolecular systems generally require resources from their host cell to function. This resource demand imposes a gene-expression burden on the host cell corresponding to the sequestration of shared cellular resources from endogenous cellular processes. Such burden typically impacts the dynamic behaviour of the cell and of the engineered biomolecular systems it hosts. The impact of burden can be severe and even cause loss of function of the designed biomolecular circuits in the cell [1].

Recently, significant attention has been given to the role of shared cellular resources in synthetic biological designs [2], [3]. The impact of resources can be further understood by developing whole-cell mathematical models, which show the interdependence of gene expression, cell growth, and resources [4]. Similarly, a quantitative understanding of host and circuit interaction through host/resource-aware modelling can help predict the performance of synthetic circuits [5]–[8] as well as highlight systems-level trade-offs that can emerge from resource constraints [9], [10]. In a cell-free system, these mathematical predictions have been used to quantify the cellular competition between synthetic genes [11]–[13], and similarly, a qualitative relationship between resources and dynamical performance has been demonstrated using a gene expression capacity monitor in living cells [2], [14].

Several approaches have been proposed to mitigate burden-imposed effects on co-expressed genes. One approach consists in designing a resource allocation controller to dynamically distribute ribosomes so as to restore modularity when heterologous genes are co-expressed [15], [16]. Other approaches focus on the use of biomolecular feedback mechanisms that respond to gene expression burden by reducing the net resource demand of synthetic genetic circuits [3], [17], or of incoherent feedforward loops designed to mitigate the impact of gene dosage on circuit performance [18]–[20]. Taking shared cellular resources explicitly into account in the design of biomolecular systems opens up new avenues for resource-aware designs that strike a balance between robust performance and efficient use of resources. A recent example of this is the design of a resource-based incoherent feedforward loop that can adapt to variations in copy number under certain conditions related to resource demand [21].

We here aim to leverage resource constraint-based interconnections to understand and tune the dynamical response in synthetically designed biomolecular circuits [22]. To this effect, in what follows, we present a coarse-grained model capturing the resource-based interactions created by shared translational resources in biomolecular circuits. We use this modelling framework to show that such interactions impact the dynamical response, paving the way for them to be used as a design tool. We then show that these resource constraints can be interpreted as a state-feedback control mechanism that can be exploited to stabilize a class of integral feedback controllers without compromising perfect adaptation.

AP is with the Department of Electrical Engineering, IIT Kanpur, India. GBS is with the Department of Bioengineering, Imperial College London, UK, e-mails: apatel@iitk.ac.in, g.stan@imperial.ac.uk

II. Results

A. Modelling resource-aware co-expression of genes

Consider a set of genes, which, when constitutively transcribed produce the corresponding mRNAs X_{mi}, with i ranging from 1 to n. The production of proteins X_{pi} from these mRNAs requires the use of the shared cellular resource R, for example Ribosome. A simple set of chemical reactions representing this gene expression process is given by

$$\begin{aligned} \phi &\xrightarrow{u_i\alpha_{mi}} X_{mi} \xrightarrow{\gamma_{mi}} \phi \\ X_{mi} + \mathrm{R} &\underset{k_i^-}{\overset{k_i^+}{\rightleftharpoons}} \mathrm{C}_i \xrightarrow{\alpha_{pi}} X_{pi} + \mathrm{R} + X_{mi} \\ X_{pi} &\xrightarrow{\gamma_{pi}} \phi \end{aligned}$$

where α_{mi} represents the production rate of X_{mi}, γ_{mi} represents the removal rate (via degradation and/or dilution) of X_{mi}, α_{pi} represents the production rate of X_{pi} and γ_{pi} represents the removal rate of X_{pi}, u_i represents the input signal to the gene expression system. For regulated gene expression, u_i is a function $f_i(x)$ of a regulating effector molecule x, while for unregulated gene expression, u_i is a constant. The value of u_i is assumed to be between 0 and 1.

Using the law of mass action, the following set of Ordinary Differential Equations can be obtained for this simple

resource-dependent gene expression system:

$$\begin{aligned}\dot{x}_{mi} &= \alpha_{mi}u_i - \gamma_{mi}x_{mi} - k_i^+ x_{mi}R + \alpha_{pi}C_i + k_i^- C_i,\\ \dot{C}_i &= k_i^+ x_{mi}R - \alpha_{pi}C_i - k_i^- C_i,\\ \dot{x}_{pi} &= \alpha_{pi}C_i - \gamma_{pi}x_{pi},\end{aligned} \tag{1}$$

where x_{mi} and x_{pi} represent the cellular concentrations of X_{mi} and X_{pi}, respectively, while R and C_i represent the cellular concentrations of the resource R and translation complex C_i.

Under the assumption that the complex dynamics is much faster compared to the dynamics of other molecular species, using time-scale separation [23], the dynamics of the cellular concentration of the complex can be assumed to be at quasi-steady-state ($\dot{C}_i \approx 0$). Hence, the model reduces to:

$$\begin{aligned}\dot{x}_{mi} &= \alpha_{mi}u_i - \gamma_{mi}x_{mi},\\ \dot{x}_{pi} &= \alpha_{pi}K_i x_{mi}R - \gamma_{pi}x_{pi},\end{aligned} \tag{2}$$

where $K_i = \dfrac{k_i^+}{\alpha_{pi} + k_i^-}$ represents the resource demand coefficient for gene i.

To capture the resource constraint, we assume that the total cellular concentration of shared resources R_T is constant. The resource can be either in the free form R or bound as part of the complex C_i. Considering these, we have:

$$\begin{aligned}R_T =& R + \sum_{j=1}^{n} C_j = R + \sum_{j=1}^{n} K_j R x_{mj} = R(1 + \sum_{j=1}^{n} K_j x_{mj})\\ \implies & R = \frac{R_T}{1 + \sum_{j=1}^{n} K_j x_{mj}}.\end{aligned} \tag{3}$$

It is interesting to note that the amount of available resource R is inversely proportional, via the resource demand coefficient K_j, to the cellular concentration of mRNA. A high value of K_j implies that the expression of gene j uses more resources, leading to a lower amount of available resources R.

Substituting R into Eq. (2), we obtain,

$$\begin{aligned}\dot{x}_{mi} &= \alpha_{mi}u_i - \gamma_{mi}x_{mi},\\ \dot{x}_{pi} &= \alpha_{pi}\frac{K_i x_{mi}}{1 + \sum_{j=1}^{n} K_j x_{mj}} R_T - \gamma_{pi}x_{pi}.\end{aligned} \tag{4}$$

As the dynamics of mRNAs is typically (much) faster compared to that of protein, we can further reduce the model using a quasi-steady-state approximation of the mRNAs dynamics (i.e. $\dot{x}_{mi} \approx 0$ when compared to the timescale of the $\dot{x}_{pi}$ species) to obtain a simplified model, which focuses exclusively on protein dynamics:

$$\dot{x}_{pi} = \alpha_{pi}\frac{K_i(\alpha_{mi}u_i/\gamma_{mi})}{1 + \sum_{j=1}^{n} K_j(\alpha_{mj}u_j/\gamma_{mj})} R_T - \gamma_{pi}x_{pi}. \tag{5}$$

B. Effect of resource constraint on dynamical behaviour

In this section, we investigate the effect of resource constraint on two important characteristics i.e. the steady-state and response time of the system described in (4), of the co-expressed genes dynamics (Fig. 1a).

The steady-state without resource constraint is given by $x_{mi,e} = \dfrac{\alpha_{mi}u_i}{\gamma_{mi}}, x_{pi,e} = \dfrac{\alpha_{pi}\alpha_{mi}}{\gamma_{pi}\gamma_{mi}}u_i K_i R$, while the steady-state with resource constraint is $x_{mi,e} = \dfrac{\alpha_{mi}u_i}{\gamma_{mi}}, x_{pi,e} = \dfrac{\alpha_{pi}\alpha_{mi}}{\gamma_{pi}\gamma_{mi}}K_i u_i \dfrac{1}{1 + \sum_{j=1}^{n} K_j \dfrac{\alpha_{mj}u_j}{\gamma_{mj}}} R_T$. R represents the concentration of resources available for the gene expression. In the case where there is no resource constraint (i.e. $K_j = 0, \forall j$), R is equal to the total concentration of resources in the cell R_T. Based on these, we note that resource constraints lead to a lower steady-state concentration of x_{pi} by a factor $\frac{1}{1+\sum_{j=1}^{n} K_j \frac{\alpha_{mj}u_j}{\gamma_{mj}}}$.

In the case of n copies of the same gene, the protein steady-state concentration for each gene copy is given by $x_{pi,e} = \dfrac{\alpha_{pi}\alpha_{mi}}{\gamma_{pi}\gamma_{mi}}K_i u_i \dfrac{1}{1 + nK_i \dfrac{\alpha_{mi}u_i}{\gamma_{mi}}} R_T$. The total protein concentration in the cell is given by $x_{pi,e}^{tot} = nx_{pi,e} = \dfrac{\alpha_{pi}\alpha_{mi}}{\gamma_{pi}\gamma_{mi}}K_i u_i \dfrac{n}{1 + nK_i \dfrac{\alpha_{mi}u_i}{\gamma_{mi}}} R_T$.

The sensitivity, i.e. the change in $x_{pi,e}^{tot}$ for a change in n, can be calculated as

$$\frac{d}{dn}x_{pi,e}^{tot} = \frac{\alpha_{pi}\alpha_{mi}}{\gamma_{pi}\gamma_{mi}}K_i u_i \frac{1}{\left(1 + nK_i \dfrac{\alpha_{mi}u_i}{\gamma_{mi}}\right)^2} R_T. \tag{6}$$

This shows that the sensitivity of total protein yield with respect to copy numbers decreases with an increase in the copy number.

To understand the timescale around these steady-states, we linearise the multiple copies model in (4) around its equilibrium point. The linearised model is given as:

$$\begin{aligned}\delta\dot{x}_{mi} &= -\gamma_{mi}\delta x_{mi},\\ \delta\dot{x}_{pi} &= \frac{\alpha_{pi}K_i R_T}{(1 + nK_i x_{mi,e})^2}\delta x_{mi} - \gamma_{pi}\delta x_{pi}.\end{aligned} \tag{7}$$

The time response of this system can be inferred by performing a convergence analysis using the Lyapunov function $V(t) = 1/2(\delta x_{mi}^2 + \delta x_{pi}^2)$. Using this Lyapunov function, we have:

$$\begin{aligned}\frac{dV}{dt} =& \delta x_{mi}\delta\dot{x}_{mi} + \delta x_{pi}\delta\dot{x}_{pi},\\ =& \begin{bmatrix}\delta x_{mi}\\ \delta x_{pi}\end{bmatrix}^T \underbrace{\begin{bmatrix}-\gamma_{mi} & \frac{K_i\alpha_{pi}R_T}{2(1+nK_i x_{mi,e})^2}\\ \frac{K_i\alpha_{pi}R_T}{2(1+nK_i x_{mi,e})^2} & -\gamma_{pi}\end{bmatrix}}_{Q} \begin{bmatrix}\delta x_{mi}\\ \delta x_{pi}\end{bmatrix}\\ \leq& \mu_1(Q)V,\end{aligned} \tag{8}$$

where $\mu_1(Q) = \sup_j\{Q_{jj} + \sum_{i\neq j}|Q_{ij}|\}$ (Q_{ij} represents the entry in the ith row and jth column of matrix Q) is the matrix measure defined in [24], which here evaluates to: $\mu_1(Q) = \max\{-\gamma_{mi} + \frac{K_i\alpha_{pi}R_T}{2(1+nK_i x_{mi,e})^2}, -\gamma_{pi} + \frac{K_i\alpha_{pi}R_T}{2(1+nK_i x_{mi,e})^2}\}$). From this, we note that, as the number of copies/genes decreases, the matrix measure increases, leading to a lower-bound slower convergence rate. This bound of convergence rate

implies the convergence rate is atleast to the value of the bounds. Similarly, if the copy number increases, we expect a faster response time. It is interesting to note that for the protein dynamics model in (5), the convergence rate would have been $-\gamma_{pi}$, i.e. independent of number of genes. However, protein dynamics in a different configuration of genes, for example in a gene cascade [22], can show a resource-constraint-dependent response time.

For cascaded gene expression systems,

$$\dot{x}_{pi} = \alpha_{pi} \frac{\bar{K}_{i-1} x_{p(i-1)}}{1 + \sum_{j=1}^{n-1} \bar{K}_j x_{pj}} R_T - \gamma_{pi} x_{pi}, \tag{9}$$

where $\bar{K}_i = \frac{\alpha_{mi} K_i}{\gamma_{mi}}, x_{p0} = 1, \bar{K}_0 = 1$. It is to be noted that denominator contains only those proteins x_{pj} which sequester resources when acting as transcription factors. The linearised model around the equilibrium point is,

$$\begin{aligned} \delta\dot{x}_{pi} = & \frac{\alpha_{pi} R_T \bar{K}_{i-1} (1 + \sum_{j \neq i-1} \bar{K}_j x_{pj,e})}{(1 + \sum \bar{K}_j x_{pj,e})^2} \delta x_{p(i-1)} \\ & - \left(\frac{\alpha_{pi} R_T \bar{K}_{i-1} \bar{K}_i x_{p,i-1,e}}{(1 + \sum \bar{K}_j x_{pj,e})^2} + \gamma_{pi} \right) \delta x_{pi} \\ & - \frac{\alpha_{pi} R_T \bar{K}_{i-1} x_{p(i-1),e}}{(1 + \sum \bar{K}_j x_{pj,e})^2} \sum_{j \neq i} \bar{K}_j \delta x_{pj}. \end{aligned} \tag{10}$$

Consider a two-node gene expression cascade where X_1 activates X_2. The mathematical model for the protein dynamics under resource constraint is,

$$\begin{aligned} \dot{x}_{p1} = & \frac{\alpha_{p1} R_T}{1 + \bar{K}_1 x_{p1}} - \gamma_{p1} x_{p1}, \\ \dot{x}_{p2} = & \frac{\alpha_{p2} \bar{K}_1 x_{p1} R_T}{1 + \bar{K}_1 x_{p1}} - \gamma_{p2} x_{p2}, \end{aligned} \tag{11}$$

where x_1 and x_2 are protein concentrations, α_{p1} and α_{p2} are the protein production rates, and γ_{p1} and γ_{p2} are the protein degradation rates of x_1 and x_2, respectively. The linearised dynamics can be written as:

$$\begin{aligned} \delta\dot{x}_{p1} = & \left(\frac{-\alpha_{p1} R_T \bar{K}_1}{(1 + \bar{K}_1 x_{p1,e})^2} - \gamma_{p1} \right) \delta x_{p1}, \\ \delta\dot{x}_{p2} = & \frac{\alpha_{p2} \bar{K}_1 R_T}{(1 + \bar{K}_1 x_{p1,e})^2} \delta x_{p1} - \gamma_{p2} \delta x_{p2}. \end{aligned} \tag{12}$$

From (12), the δx_{p1} dynamics has convergence rate of $\frac{-\alpha_{p1} R_T \bar{K}_1}{(1+\bar{K}_1 x_{p1})^2} - \gamma_{p1}$ due to the resource constraint whereas without resource constraint the convergence rate is $-\gamma_{p1}$. This increase results in faster response of the dynamics.

We note that resource coefficients act as feedback gains from other mRNA states. As the number of gene increases the negative feedback strength increases, which operates in a similar manner to a negative feedback genetic circuit. It is well known that negative feedback in genetic circuit decreases the steady-state and reduces the response time of the output protein concentration [25]. To verify this, we simulated the model for different the number of genes. We note that as the number of genes increases, the steady-state value decreases as expected (Fig. 1b). Furthermore, we also observe that the response time also decreases with an increase in the number of genes (Fig. 1c). This decrease is not linearly proportional to the increase in the number of genes. This can be understood from the matrix measure in (8), where the change due to resource constraint is $\Delta = \frac{K_i}{2(1+nK_i x_{mi,e})^2}$. The sensitivity of this matrix measure to the number of genes can be computed as $\frac{d\Delta}{dn} = \frac{-K_i^2 x_{mi,e}}{(1+nK_i x_{mi,e})}$. This sensitivity decreases as the number of genes increases. To further show the difference in response time, we compare in Fig. 1d the response time for the cases with $n = 10$ co-expressed genes with and without resource constraint.

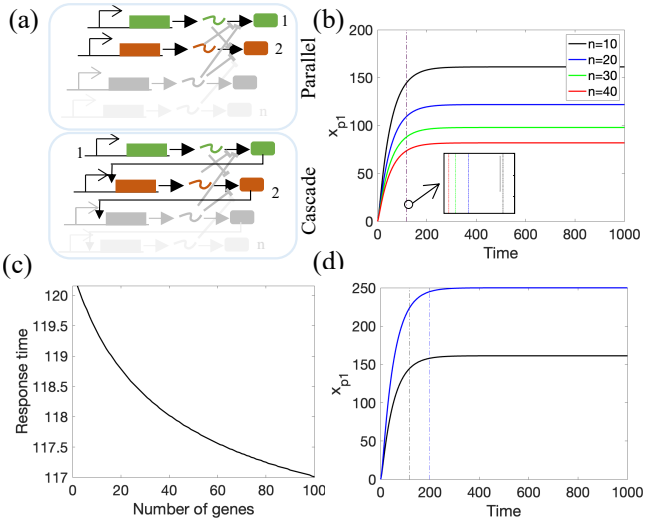

Fig. 1. (a) Schematic of co-expressed (parallel) genes and cascaded genes, where the impact of resource constraints are shown as unintended interactions. (b) Expression dynamics of a protein of interest when several additional genes are co-expressed. This shows that as the number of genes increases, the steady-state level of the protein of interest decreases. The simulation parameters are $\alpha_{mi} = 1nM/min$, $\alpha_{pi} = 1nM/min$, $\gamma_{mi} = 0.2\ 1/min$, $\gamma_{pi} = 0.1\ 1/min$, $R_T = 100$, $K_i = 0.01$. (c) Response time (defined as the time required to reach 90% of the steady-state value) as a function of the number of co-expressed genes. d) The blue line represents the case of gene expression without any resource constraint, while the black line represents the case of gene expression under resource constraint. The dashed vertical lines indicate the time taken for the concentration of the protein of interest to reach 90% of its steady-state value (also known as response time). For both the cases, the total number of genes $n = 10$.

C. Fold-change detection in Incoherent Feedforward Loops

To investigate whether resource constraints can impact the qualitative behaviour of gene networks different from those discussed in the previous section, we consider an incoherent feedforward loop (iFFL). iFFLs constitute a commonly used biological motif for step input disturbance rejection and fold-change detection as their temporal responses are identical for input step signals exhibiting the same fold change. The gene network architecture of an iFFL can be described as follows: an external input u activates two genes X_1 and X_2, while the protein expressed from gene X_1 acts as a repressor for the expression of gene X_2 (Fig. 2b, inset).

A standard resource-agnostic model for an incoherent feedforward loop is given as [26]:

$$\begin{aligned}\dot{x}_{p1} &= \alpha_{p1}u - \gamma_{p1}x_{p1},\\ \dot{x}_{p2} &= \alpha_{p2}u\frac{K}{x_{p1}} - \gamma_{p2}x_{p2}.\end{aligned} \tag{13}$$

where x_{p1} and x_{p2} are protein concentrations for genes X_1 and X_2, respectively. K is the DNA binding constant of X_1 to the promoter of X_2, α_{p1} is the translation rate for the protein of gene X_1, γ_{p1} is the degradation rate for the protein of gene X_1, α_{p2} is the translation rate for the protein of gene X_2, and γ_{p2} is the degradation rate for the protein of gene X_2.

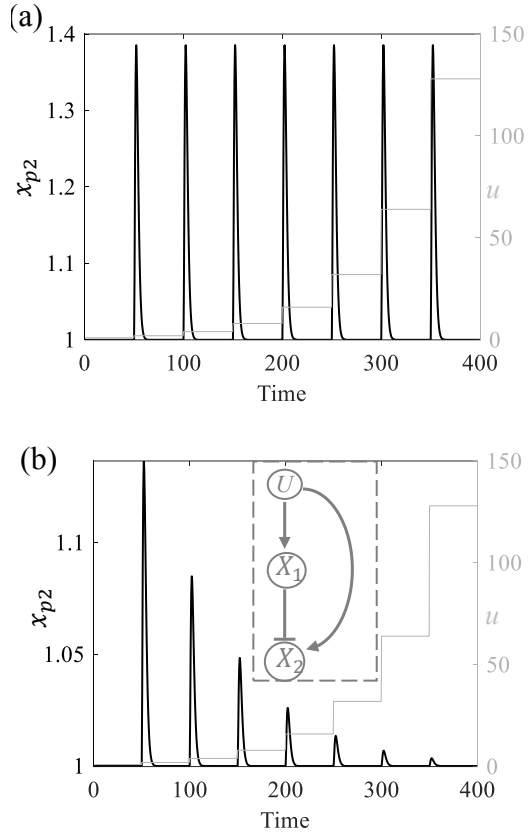

Fig. 2. Standard model response (a) and resource constraint model response (b) for a stair case of step signals (light grey). The input signal u starts with a normalised value of 1 and increases by two fold at regular time intervals. The parameters for the simulations are $\alpha_{p1} = 100\ nM/hr$, $\alpha_{p2} = 100\ nM/hr$, $\gamma_{p1} = 1\ 1/hr$, $\gamma_{p2} = 1\ 1/hr$, $K = 1$.

In what follows, this model is simulated considering a stair case of step signals applied at the iFFL input u, with the fold change between consecutive steps kept constant. When considering such a model of the iFFL, i.e. a model which doesn't take into account limited resources for gene expression, one can observe that the output response remains identical as long as the step fold change remains the same, irrespective of the absolute values of u (Fig. 2a).

Similarly to what we did in Section II-A, if one takes into account consumption of shared cellular resources during co-expression of genes, the model becomes:

$$\begin{aligned}\dot{x}_{p1} &= \alpha_{p1}\frac{\bar{K}_u u}{1+\bar{K}_u u+\bar{K}_1 x_{p1}} - \gamma_{p1}x_{p1},\\ \dot{x}_{p2} &= \alpha_{p2}\frac{\bar{K}_u u}{1+\bar{K}_u u+\bar{K}_1 x_{p1}}\frac{K}{x_{p1}} - \gamma_{p2}x_{p2}.\end{aligned} \tag{14}$$

When simulated for the same stair case step input as for Figure 2.(a), we observe that the response retains the adaptation property but loses fold change detection ability (Fig. 2b). This change in the dynamics is due to resource constraints. A high absolute value of u generates a larger pool of mRNA and demands more resources to produce the protein. From a previously reported mathematical condition for fold change detection [27], in a system represented as

$$\begin{aligned}\dot{x} &= f(x,y,u),\\ \dot{y} &= g(x,y,u),\end{aligned} \tag{15}$$

(here, $x = x_{p1}$ and $y = x_{p2}$) fold-change detection is guaranteed if the system is stable and the following homogeneity conditions, are met for all positive values of a parameter r:

$$\begin{aligned}f(rx,y,pu) &= rf(x,y,u),\\ g(rx,y,pu) &= g(x,y,u). \quad \forall r>0\end{aligned} \tag{16}$$

We can see that, while the model in (13) meets these conditions, the model in (14) does not meet them. However, both these models retain the adaptation property.

D. Stabilization of the antithetic integral feedback controller

A key mechanism for guaranteeing robust perfect adaptation (robust zero steady-state error) consists in the use of negative integral feedback. It has been shown that a special class of integral controllers, known as antithetic integral controllers (AICs), can be implemented biomolecularly to that effect [28]. The robust performance of antithetic integral controllers is guaranteed only when the closed-loop system dynamics is asymptotically stable and the sole means of removal/inactivation of the antithetic controller molecules from the system is by reacting with themselves (i.e. zero-order degradation for the antithetic controller molecules). Although additional biomolecular controllers can be engineered to ensure stability, this comes at the cost of additional complexity and demand for cellular resources.

In what follows, we consider a simple reaction network consisting of two species: a controlled species X_1, and an output species X_2, with X_1 promoting the expression of X_2. An AIC consisting of the molecular species Z_1 and Z_2 is connected to this simple reaction network with the aim to robustly control the steady-state level of the output species X_2. The typical structure of the antithetic controller for this set of two genes (X_1 and X_2) is depicted in Fig. 3(a), where Z_1 actuates X_1, and Z_2 senses X_2. In the ideal setting, the AIC species Z_1 and Z_2 can only be removed from the system by binding to each other at a rate η, thereby forming an inactive complex.

Without accounting for consumption of shared cellular resources, the dynamics of this prototypical closed-loop

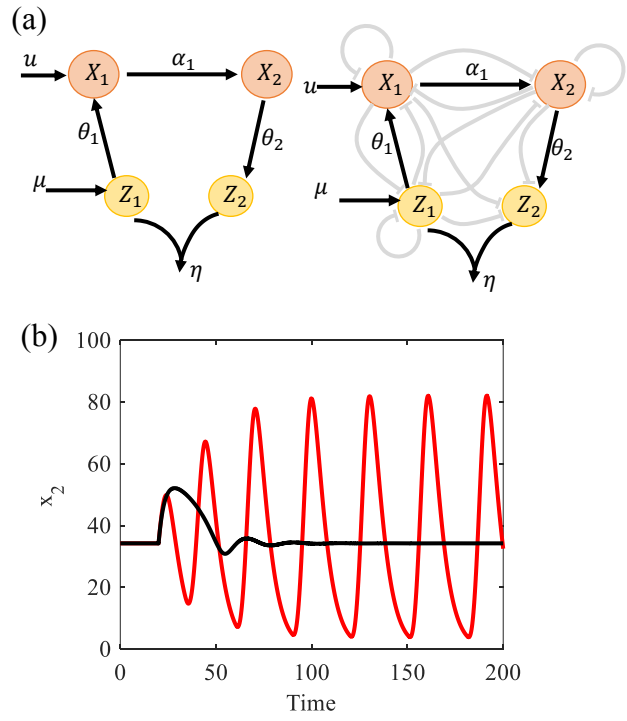

Fig. 3. (a) Schematic of an antithetic integral controller (Z_1, Z_2) connected to a simple reaction network (X_1, X_2). Due to resource constraints, additional interactions arise. Explicit regulatory interconnections are represented in black, while implicit resource-induced interconnections are represented in grey. (b) The red trace indicates the time evolution of the concentration of x_2 without resource constraints while the black trace indicates the time evolution of x_2 when resource constraints are considered for the same parameter set and step change in u. The parameters considered for simulations are α_1=0.1125 au, γ_1=0.2817 au, γ_2=0.2062 au,θ_1=1.6321 au θ_2=0.2364 au, η=5.7490 au, μ=8.0898 au.

system is given as [29]:

$$\begin{aligned}\frac{dx_1}{dt} &= \theta_1 u z_1 - \gamma_1 x_1,\\ \frac{dx_2}{dt} &= \alpha_1 x_1 - \gamma_2 x_2,\\ \frac{dz_1}{dt} &= \mu - \eta z_1 z_2,\\ \frac{dz_2}{dt} &= \theta_2 x_2 - \eta z_1 z_2,\end{aligned} \tag{17}$$

where x_1, x_2, z_1, and z_2 represent the concentrations of the species X_1, X_2, Z_1, and Z_2, respectively. θ_1, θ_2, α_1 are the production rates of x_1, z_2, and x_2, respectively. η is the rate at which z_1 and z_2 bind to and sequester each other. γ_1, γ_2 are degradation rates of x_1, and x_2, respectively. μ is the production rate of z_1 providing the reference signal. Here, u is the disturbance input against which adaptation is sought by the antithetic integral controller.

At steady-state, *if the closed-loop system is stable*, $x_2 = \frac{\mu}{\theta_2}$ [29]. This steady-state value is independent of u as well as the parameters α_1, θ_1, and η, making it robust against perturbations to these parameters.

It has been observed that in certain parameter regimes the feedback system looses stability [30], [31]. In such cases, its critical to consider design aspects that can stabilize the closed-loop system.

In the presence of resource constraint, the dynamical model of the closed-loop system becomes,

$$\begin{aligned}\frac{dx_1}{dt} &= \theta_1\ u\frac{J_1 z_1}{1+K_1x_1+K_2x_2+J_1z_1} - \gamma_1 x_1,\\ \frac{dx_2}{dt} &= \alpha_1\frac{K_1 x_1}{1+K_1x_1+K_2x_2+J_1z_1} - \gamma_2 x_2,\\ \frac{dz_1}{dt} &= \mu\frac{1}{1+K_1x_1+K_2x_2+J_1z_1} - \eta z_1 z_2,\\ \frac{dz_2}{dt} &= \theta_2\frac{K_2 x_2}{1+K_1x_1+K_2x_2+J_1z_1} - \eta z_1 z_2,\end{aligned} \tag{18}$$

where K_1, K_2, and J_1 are the resource demand coefficients.

These additional interactions have the potential to induce stability or enlarge the parameter ranges for which the closed-loop system is stable.

To investigate the stability of the closed loop system, we linearize the system dynamics around its equilibrium point. The linearized dynamics is given by:

$$\begin{bmatrix}\delta\dot{x}_1\\ \delta\dot{x}_2\\ \delta\dot{z}_1\\ \delta\dot{z}_2\end{bmatrix} = \begin{bmatrix}-\gamma_1 & 0 & \theta_1 u J_1 q & 0\\ \alpha_1 K_1 q & -\gamma_2 & 0 & 0\\ 0 & 0 & -\eta z_{2,e} & -\eta z_{1,e}\\ 0 & \theta_2 K_2 q & -\eta z_{2,e} & -\eta z_{1,e}\end{bmatrix}\begin{bmatrix}\delta x_1\\ \delta x_2\\ \delta z_1\\ \delta z_2\end{bmatrix} +$$
$$\begin{bmatrix}-\theta_1 u J_1 z_{1,e} K_1 q^2 & -\theta_1 u J_1 z_{1,e} K_2 q^2 & -\theta_1 u J_1 z_{1,e} K_1 q^2 & 0\\ -\alpha_1 K_1^2 x_{1,e} K_1 q^2 & -\alpha_1 K_1 x_{1,e} K_2 q^2 & -\alpha_1 K_1 x_{1,e} J_1 q^2 & 0\\ -\mu K_1 q^2 & -\mu K_2 q^2 & -\mu J_1 q^2 & 0\\ -\theta_2 K_2 x_{2,e} K_1 q^2 & -\theta_2 K_2^2 x_{2,e} q^2 & -\theta_2 K_2 x_{2,e} J_1 q^2 & 0\end{bmatrix}\begin{bmatrix}\delta x_1\\ \delta x_2\\ \delta z_1\\ \delta z_2\end{bmatrix}$$
$$= \underbrace{\begin{bmatrix}-\gamma_1 & 0 & \theta_1 u J_1 q & 0\\ \alpha_1 K_1 q & -\gamma_2 & 0 & 0\\ 0 & 0 & -\eta z_{2,e} & -\eta z_{1,e}\\ 0 & \theta_2 K_2 q & -\eta z_{2,e} & -\eta z_{1,e}\end{bmatrix}}_{A}\begin{bmatrix}\delta x_1\\ \delta x_2\\ \delta z_1\\ \delta z_2\end{bmatrix}$$
$$- q^2 \underbrace{\begin{bmatrix}\theta_1 u J_1 z_{1,e}\\ \alpha_1 K_1 x_{1,e}\\ \mu\\ \theta_2 K_2 x_{2,e}\end{bmatrix}}_{B}\underbrace{\begin{bmatrix}K_1 & K_2 & J_1 & 0\end{bmatrix}}_{K}\begin{bmatrix}\delta x_1\\ \delta x_2\\ \delta z_1\\ \delta z_2\end{bmatrix},$$

where $q = \dfrac{1}{1+K_1x_{1,e}+K_2x_{2,e}+J_1z_{1,e}}$ and $\left[x_{1,e}, x_{2,e}, z_{1,e}, z_{2,e}\right]^T$ is the vector of steady-state values.

Denoting $\delta X = \begin{bmatrix}\delta x_1 & \delta x_2 & \delta z_1 & \delta z_2\end{bmatrix}^T$, the linearised system dynamics can be compactly rewritten as,

$$\delta\dot{X} = A\delta X - q^2 BK\delta X = (A - q^2 BK)\delta X = A_r\delta X, \tag{19}$$

with $A_r = A - q^2 BK$. Interestingly, this feedback structure is very close to the structure of a state feedback controller. Note that the resource-aware model retains the adaptation property of the antithetic controller since $x_{2,e} = \dfrac{\mu}{K_2\theta_2}$. We observe that this steady-state value is dependent on the additional parameter K_2. This is expected as K_2 is the resource coefficient related X_2 and acts as a scaling factor of θ_2 in the model.

Proposition 1. *The equilibrium point of* (18) *can be made stable, i.e. A_r is Hurwitz, if the resource demand J_1 satisfies* $J_1 < \frac{1}{2z_{1e}q}$.

Proof. The closed-loop system matrix $A_r = A - q^2BK$ is given by:

$$A_r = \underbrace{\begin{bmatrix} -\gamma_1 & 0 & 0 & 0 \\ \alpha_1 K_1 q & -\gamma_2 & 0 & 0 \\ 0 & 0 & -\eta z_{2,e} & -\eta z_{1,e} \\ 0 & \theta_2 K_2 q & -\eta z_{2,e} & -\eta z_{1,e} \end{bmatrix}}_{A_0} +$$

$$\underbrace{\begin{bmatrix} -\theta_1 u J_1 z_{1,e} K_1 q^2 & -\theta_1 u J_1 z_{1,e} K_2 q^2 & -\theta_1 u J_1 z_{1,e} K_1 q^2 + \theta_1 u J_1 q & 0 \\ -\alpha_1 K_1^2 x_{1,e} K_1 q^2 & -\alpha_1 K_1 x_{1,e} K_2 q^2 & -\alpha_1 K_1 x_{1,e} J_1 q^2 & 0 \\ -\mu K_1 q^2 & -\mu K_2 q^2 & -\mu J_1 q^2 & 0 \\ -\theta_2 K_2 x_{2,e} K_1 q^2 & -\theta_2 K_2^2 x_{2,e} q^2 & -\theta_2 K_2 x_{2,e} J_1 q^2 & 0 \end{bmatrix}}_{\Delta A}$$

The matrix A_0 has its rightmost eigenvalue at 0. Perturbation of A_0 by the matrix ΔA determines the overall local asymptotic stability of the steady-state. We use the perturbation theory from [32], [33] to characterise the local stability of A_r by considering the value of the drift of the zero eigenvalue of A_0. The perturbation in the zero eigenvalue is $\Delta\lambda = u^T \Delta A v + O(\Delta A)$, where $u^T = \begin{bmatrix} \underbrace{\frac{\alpha_1 K_1 K_2 \theta_2 q^2}{\gamma_1 \gamma_2}}_{u_1} & \underbrace{\frac{K_2 \theta_2 q}{\gamma_2}}_{u_2} & -1 & 1 \end{bmatrix}$ is the left eigenvector of A_0, and $v^T = \begin{bmatrix} 0 & 0 & -z_{1,e} & z_{2,e} \end{bmatrix}$ is the right eigenvector of A_0.

$$\begin{aligned}
\Delta\lambda =& u^T \Delta A v \\
=& \begin{bmatrix} u_1 \\ u_2 \\ -1 \\ 1 \end{bmatrix}^T \Delta A \begin{bmatrix} 0 \\ 0 \\ -z_1 \\ z_2 \end{bmatrix} \\
=& \begin{bmatrix} u_1 \\ u_2 \\ -1 \\ 1 \end{bmatrix}^T \begin{bmatrix} \theta_1 u J_1^2 z_{1,e}^2 q^2 - \theta_1 u J_1 q z_{1,e} \\ \alpha_1 K_1 x_{1,e} J_1 q^2 z_{1,e} \\ \mu J_1 q^2 z_{1,e} \\ \theta_2 K_2 x_{2,e} J_1 q^2 z_{1,e} \end{bmatrix} \\
=& \begin{bmatrix} u_1 \\ u_2 \\ -1 \\ 1 \end{bmatrix}^T \begin{bmatrix} \theta_1 u J_1^2 z_{1,e}^2 q^2 - \theta_1 u J_1 q z_{1,e} \\ \alpha_1 K_1 x_{1,e} J_1 q^2 z_{1,e} \\ \mu J_1 q^2 z_{1,e} \\ \mu J_1 q^2 z_{1,e} \end{bmatrix} \quad (x_{2,e} = \frac{\mu}{\theta_2 K_2}) \\
=& \theta_1 u J_1 q z_{1,e} u_1 (J_1 z_{1,e} q - 1) + \alpha_1 K_1 x_{1,e} J_1 q^2 z_{1,e} u_2 \\
=& \theta_1 u J_1 q z_{1,e} \frac{\alpha_1 K_1 K_2 \theta_2 q^2}{\gamma_1 \gamma_2} (J_1 z_{1,e} q - 1) \\
& + \alpha_1 K_1 x_{1,e} J_1 q^2 z_{1,e} \frac{K_2 \theta_2 q}{\gamma_2} \\
=& \frac{J_1 q^3 \alpha_1 K_1 K_2 \theta_2}{\gamma_2} \left[(J_1 z_{1,e} q - 1) \frac{\theta_1 u}{\gamma_1} + x_{1,e} \right] \\
=& \frac{J_1 q^3 \alpha_1 K_1 K_2 \theta_2}{\gamma_2} \left[(J_1 z_{1,e} q - 1) \frac{\theta_1 u}{\gamma_1} + \frac{J_1 z_{1,e} u \theta_1 q}{\gamma_1} \right].
\end{aligned} \tag{20}$$

For sufficiently small values of J_1, i.e. $J_1 < \frac{1}{2 z_{1,e} q}$, we have $-\frac{\theta_1 u}{\gamma_1} + \frac{2 J_1 z_{1,e} u \theta_1 q}{\gamma_1} < 0$ and as a consequence the eigenvalue drift is negative. Under this assumption, the closed-loop matrix A_r is Hurwitz. □

This condition can be physically interpreted as follow. The resource demand for the expression of x_1, J_1, should be sufficiently small, implying the use of a lean biomolecular controller. As the dynamics of z_1 is assumed to be free of first order degradation, any instability in the dynamics of x_1 is scaled down by J_1. Therefore, when J_1 satisfies the condition $J_1 < \frac{1}{2 z_{1,e} q}$, J_1 becomes inversely related to the steady-state value of z_1.

We consider a situation for which the fixed point of the closed-loop system is unstable and the system exhibits an oscillatory behaviour around this fixed point (Fig. 3(b), red trace). However, shown that when resource constraints are accounted for and the resource demand coefficients are chosen as per proposition 1, the equilibrium point is locally asymptotically stable and perfect adaptation is restored (Fig. 3(b), black trace).

III. Discussion

A conventional approach to control the dynamical behaviour of gene networks is through the design of biomolecular feedback control systems that act upon them. The function of these biomolecular control systems requires consumption of shared cellular resources, which are often not taken into account explicitly. Resource limitation typically couples different co-expressed genes in such a way that overexpression of a gene leads to reduced expression of other genes. Similar to transcriptional negative feedback circuit, this resource-constraint feedback can accelerate the system response at the cost of reduced steady-state values. Further, we have shown that resource constraints can alter the qualitative behaviour of gene regulatory networks such as fold change detection in incoherent feedforward loop or coupling from upstream to downstream genes in gene expression cascades. Finally, we have shown that resource-constraint-based feedback can be approximated to a state-feedback controller design. We used this to achieve stabilization in an, otherwise unstable, antithetic integral feedback system. These preliminary results open up possibilities for the resource-aware design of biomolecular controllers.

IV. Acknowledgments

GBS gratefully acknowledges the support of the UK Royal Academy of Engineering via the Chair in Emerging Technologies for Engineering Biology (RAEng CiET 1819\5). AP would like to acknowledge the support as Early Career Fellowship by DBT/Wellcome Trust India Alliance.

References

[1] E.-M. Nikolados, A. Y. Weiße, F. Ceroni, and D. A. Oyarzún, "Growth defects and loss-of-function in synthetic gene circuits," *ACS synthetic biology*, vol. 8, no. 6, pp. 1231–1240, 2019.

[2] F. Ceroni, R. Algar, G.-B. Stan, and T. Ellis, "Quantifying cellular capacity identifies gene expression designs with reduced burden," *Nature methods*, vol. 12, no. 5, p. 415, 2015.

[3] F. Ceroni, A. Boo, S. Furini, T. E. Gorochowski, O. Borkowski, Y. N. Ladak, A. R. Awan, C. Gilbert, G.-B. Stan, and T. Ellis, "Burden-driven feedback control of gene expression," *Nature methods*, vol. 15, no. 5, pp. 387–393, 2018.

[4] A. Y. Weiße, D. A. Oyarzún, V. Danos, and P. S. Swain, "Mechanistic links between cellular trade-offs, gene expression, and growth," *Proceedings of the National Academy of Sciences*, vol. 112, no. 9, pp. E1038–E1047, 2015.

[5] C. Liao, A. E. Blanchard, and T. Lu, "An integrative circuit–host modelling framework for predicting synthetic gene network behaviours," *Nature microbiology*, vol. 2, no. 12, pp. 1658–1666, 2017.

[6] E. Atkinson, Z. Tuza, G. Perrino, G.-B. Stan, and R. Ledesma-Amaro, "Resource-aware whole-cell model of division of labour in a microbial consortium for complex-substrate degradation," *Microbial cell factories*, vol. 21, no. 1, pp. 1–12, 2022.

[7] E.-M. Nikolados, A. Y. Weiße, and D. A. Oyarzún, "Prediction of cellular burden with host–circuit models," in *Synthetic Gene Circuits*, pp. 267–291, Springer, 2021.

[8] C. D. McBride and D. Del Vecchio, "Predicting composition of genetic circuits with resource competition: demand and sensitivity," *ACS Synthetic Biology*, vol. 10, no. 12, pp. 3330–3342, 2021.

[9] A. Gyorgy and D. Del Vecchio, "Limitations and trade-offs in gene expression due to competition for shared cellular resources," in *53rd IEEE Conference on Decision and Control*, pp. 5431–5436, IEEE, 2014.

[10] T. E. Gorochowski, I. Avcilar-Kucukgoze, R. A. Bovenberg, J. A. Roubos, and Z. Ignatova, "A minimal model of ribosome allocation dynamics captures trade-offs in expression between endogenous and synthetic genes," *ACS synthetic biology*, vol. 5, no. 7, pp. 710–720, 2016.

[11] A. Gyorgy and R. M. Murray, "Quantifying resource competition and its effects in the tx-tl system," in *2016 IEEE 55th Conference on Decision and Control (CDC)*, pp. 3363–3368, IEEE, 2016.

[12] D. Siegal-Gaskins, V. Noireaux, and R. M. Murray, "Biomolecular resource utilization in elementary cell-free gene circuits," in *2013 American Control Conference*, pp. 1531–1536, IEEE, 2013.

[13] O. Borkowski, C. Bricio, M. Murgiano, B. Rothschild-Mancinelli, G.-B. Stan, and T. Ellis, "Cell-free prediction of protein expression costs for growing cells," *Nature communications*, vol. 9, no. 1, pp. 1–11, 2018.

[14] A. Gyorgy, J. I. Jiménez, J. Yazbek, H.-H. Huang, H. Chung, R. Weiss, and D. Del Vecchio, "Isocost lines describe the cellular economy of genetic circuits," *Biophysical journal*, vol. 109, no. 3, pp. 639–646, 2015.

[15] A. P. Darlington, J. Kim, J. I. Jiménez, and D. G. Bates, "Engineering translational resource allocation controllers: mechanistic models, design guidelines, and potential biological implementations," *ACS Synthetic Biology*, vol. 7, no. 11, pp. 2485–2496, 2018.

[16] A. P. Darlington, J. Kim, J. I. Jiménez, and D. G. Bates, "Dynamic allocation of orthogonal ribosomes facilitates uncoupling of co-expressed genes," *Nature communications*, vol. 9, no. 1, pp. 1–12, 2018.

[17] A. Hamadeh and D. Del Vecchio, "Mitigation of resource competition in synthetic genetic circuits through feedback regulation," in *53rd IEEE Conference on Decision and Control*, pp. 3829–3834, IEEE, 2014.

[18] R. D. Jones, Y. Qian, V. Siciliano, B. DiAndreth, J. Huh, R. Weiss, and D. Del Vecchio, "An endoribonuclease-based feedforward controller for decoupling resource-limited genetic modules in mammalian cells," *Nature communications*, vol. 11, no. 1, pp. 1–16, 2020.

[19] T. Frei, F. Cella, F. Tedeschi, J. Gutiérrez, G.-B. Stan, M. Khammash, and V. Siciliano, "Characterization and mitigation of gene expression burden in mammalian cells," *Nature communications*, vol. 11, no. 1, pp. 1–14, 2020.

[20] C. Barajas, H.-H. Huang, J. Gibson, L. Sandoval, and D. Del Vecchio, "Feedforward ribosome control mitigates gene activation burden," *bioRxiv*, 2022.

[21] G. Perrino and G.-B. Stan, "Robust set-point regulation of gene expression using resource competition couplings in mammalian cells," in *2022 American Control Conference (ACC)*, pp. 1373–1378, IEEE, 2022.

[22] Y. Qian, H.-H. Huang, J. I. Jiménez, and D. Del Vecchio, "Resource competition shapes the response of genetic circuits," *ACS Synthetic Biology*, vol. 6, no. 7, pp. 1263—-1272, 2017.

[23] D. Del Vecchio and J.-J. E. Slotine, "A contraction theory approach to singularly perturbed systems," *IEEE Transactions on Automatic Control*, vol. 58, no. 3, pp. 752–757, 2012.

[24] M. Vidyasagar, "On matrix measures and convex liapunov functions," *Journal of Mathematical Analysis and Applications*, vol. 62, no. 1, pp. 90–103, 1978.

[25] N. Rosenfeld, M. B. Elowitz, and U. Alon, "Negative autoregulation speeds the response times of transcription networks," *Journal of molecular biology*, vol. 323, no. 5, pp. 785–793, 2002.

[26] L. Goentoro, O. Shoval, M. W. Kirschner, and U. Alon, "The incoherent feedforward loop can provide fold-change detection in gene regulation," *Molecular Cell*, vol. 36, no. 5, pp. 894–899, 2009.

[27] O. Shoval, L. Goentoro, Y. Hart, A. Mayo, E. Sontag, and U. Alon, "Fold-change detection and scalar symmetry of sensory input fields," *Proceedings of the National Academy of Sciences*, vol. 107, no. 36, pp. 15995–16000, 2010.

[28] S. K. Aoki, G. Lillacci, A. Gupta, A. Baumschlager, D. Schweingruber, and M. Khammash, "A universal biomolecular integral feedback controller for robust perfect adaptation," *Nature*, vol. 570, no. 7762, pp. 533–537, 2019.

[29] C. Briat, A. Gupta, and M. Khammash, "Antithetic integral feedback ensures robust perfect adaptation in noisy biomolecular networks," *Cell systems*, vol. 2, no. 1, pp. 15–26, 2016.

[30] A.-A. Baetica, Y. P. Leong, and R. M. Murray, "Guidelines for designing the antithetic feedback motif," *Physical Biology*, vol. 17, no. 5, p. 055002, 2020.

[31] N. Olsman, A.-A. Baetica, F. Xiao, Y. P. Leong, R. M. Murray, and J. C. Doyle, "Hard limits and performance tradeoffs in a class of antithetic integral feedback networks," *Cell systems*, vol. 9, no. 1, pp. 49–63, 2019.

[32] A. P. Seyranian and A. A. Mailybaev, *Multiparameter stability theory with mechanical applications*, vol. 13. World Scientific, 2003.

[33] C. Briat and M. Khammash, "On the innocuousness of deterministic p-type antithetic integral controllers arising in integral rein control," *arXiv preprint arXiv:2201.13375*, 2022.